Constant Stress Arches and their Design Space

Wanda J. Lewis
School of Engineering, University of Warwick
Coventry CV4 7AL, UK
Email: W.J.Lewis@warwick.ac.uk

It is generally accepted that an optimal arch has a funicular (moment-less) form and least weight. However, the feature of least weight restricts the design options and raises the question of durability of such structures. The work presented here shows that arches of least weight are just a sub-set of constant stress arches discussed here. Building on the analytical form-finding approach presented in [1], this study gives a complete description of two-pin arches that are moment-less and of constant axial stress along their entire length, when subjected to permanent (statistically prevalent) load. The theory considers a general case of an asymmetric arch, deriving the equation of its centre-line profile, horizontal reactions, and varying cross-section area. The analysis of symmetric arches follows, with the equation for the span/rise ratio minimising the arch volume being derived. It is shown that a previously claimed limit on arch span is always satisfied. Newly found limits, determining the existence of constant stress arches, lead to a concept of the design space. In the case of stand-alone arches, the design space takes the form of a constraint relationship between constant stress and span/rise ratio.

Keywords: constant stress arch, design space, moment-less arch, form-finding

1. Introduction

(a) Background and scope

The analysis presented here is inspired by the observation that the principle of constant stress, governing the formation of natural objects, such as trees, bones, or shells produces minimal response to loading. This has implications for their durability and economy of material usage. These natural structures are optimised for statistically prevalent loads and, when subjected to significant and persistent live loads, produce adaptive to maintain the state of constant stress (Mattheck [2]). Otto [3] dedicated his life to studying natural forms and developing experimental form-finding methods that shaped structures using forces applied to them. The extensive research program completed by him and his team demonstrated that form-found structures are optimal in terms of their function, economy of material usage, and aesthetic quality. The overall conclusion was that the path to defining optimal structures had its roots in nature. Alongside the experimental form-finding work, computational form-finding methods predicting shapes of a variety of structures were developed, as described in [4].

This paper builds on the contribution made in [1] describing moment-less arch forms of constant cross-section; it proposes moment-less arch forms characterised by constant axial stress along their entire length, when subjected to permanent (statistically prevalent) load. The motivation to use a constant stress principle in conjunction with permanent load to shape the arches, is drawn from nature. Through the absence of transverse shear necessary to obtain a bending-free action, the arches become statically determinate. The theory considers the

general case of an asymmetric arch configuration, from which a symmetric form is deduced. The asymmetry is produced by having arch supports placed at different levels. However, the bulk of the paper is devoted to a symmetric form to enable meaningful comparisons with previous work.

Unlike some approaches discussed below, the methodology presented here provides a complete description of the arch geometry, its reactions, and limiting factors. It shows that arches of least weight, which tend to be the main objective of structural optimisation, are just a special case of constant stress, moment-less forms. The work addresses a number of design aspects, at the forefront of which is the question of the existence of constant stress arches leading to a new concept of the design space. It is shown that, in the case of a stand-alone arch, this concept takes on a new meaning, in the form of a constraint relationship between constant stress and span/rise ratio.

The analytical form-finding approach presented here makes a clear distinction between the independent input variables: span, rise, loading, and constant value of stress, and the dependent output variables: horizontal reaction, centre line profile, and material distribution in the structure.

The main advantage of an analytical approach over a computational one is its ability to generate a family of moment-less arches just by changing a few input parameters. It also produces smooth structural profiles – a feature that, in a computational model, would require a high level of discretisation, adding to computational effort. In view of this, and with the plethora of papers published on optimal arch structures, literature review presented below is limited to analytical studies.

(b) Past work

The work on constant stress arches presented here has interesting parallels in other fields of study, which, broadly, fall into two diverse areas: suspension bridges, and structural optimization.

(i) Suspension bridge research

Early work on suspension bridges generated a lot of interest in the shape of suspension chains supporting the structure. In the 17th century it became known that the shape of a funicular (moment-less) arch was that of an 'inverted suspension chain' – an analogy first demonstrated by Robert Hooke. His demonstration was limited to showing that the curve created by a hanging chain, when inverted, gives a suitable shape of a free-standing, constant cross-section arch, supporting its own weight. The mathematical description of the curve came later, referring to it as a catenary, expressed by a hyperbolic cosine function. The theoretical work that followed focused on the derivation of a curve adopted by a suspension chain working in constant stress under its own weight. The first contribution in this area was due to by Gilbert [5] who described the curve as a 'catenary of equal strength'. His derivation, given in Newton's fluxional calculus notation, and characterised by many divergences from contemporary terminology, was made accessible by Calladine [6]. A more concise form of the 'catenary of equal strength' equation, given in Cartesian co-ordinates, was later derived by Routh [7]. A more recent exposition of the role of the inverted suspension chain (or cable) analogy in describing moment-less forms of stand-alone arches is given in [4] and [8]. The analysis presented in [4] includes an example of the iconic Gateway Arch in St. Louis, the shape of which was described by the designer, Eero Saarinen, as 'weighted catenary', due to the varying cross-section of the structure.

The early work on the 'catenary of equal strength' ([5], [7]) was of limited value to the design of suspension and arch bridges, as it did not consider the presence of the deck weight. As far as the suspension bridges are concerned, this issue was addressed by Mosely [9] who re-formulated the hanging chain equation for the combined chain and deck weight and called it 'equation to the suspension chain of uniform strength'. Although the solution was somewhat convoluted, with the chain configuration expressed in terms of the varying tension force in the structure, the inverse form of the equation for the centre-line profile matched that of a constant stress arch. However, the work, again, has a limited relevance to moment-less arch structures, as the span/rise ratio – one of the key factors defining their design space forms - lies outside that used in suspension bridges. Furthermore, with only a symmetric case being considered, it is not possible to deduce an asymmetric form. Finally, in common with the 'catenary of equal strength' and other approaches, the work uses a permissible stress value, corresponding to an ultimate, rather than permanent, load - a point discussed in Section (iii).

(ii) Structural optimisation research

Within the discipline of structural optimisation, there is a considerable amount of literature dedicated to optimal arches, referred to as moment-less (funicular) structures of least weight. The work has its origin in the studies of optimal structural layouts of trusses and frames, as shown in [10], which drew on the work of Maxwell [11] and Mitchell [12]. Later, the work progressed to weight/cost minimisation of arch and cable structures. Hill *et al* [13] derived profiles of 'fully stressed' arches, minimising the total weight of the arch subject to the constant uniform (permissible) stress along its entire its entire length. The work showed that the centre-line profile of the arch is unaffected by the external uniformly distributed load (deck weight). Led by the work of Hill *et* al [13], Wang *et al* [14] derived centre-line profiles of a number of funicular arches of least weight, including asymmetric and symmetric forms under a uniformly distributed external load and arch weight. Focusing just on structural layouts, the work did not produce an expression for the cross-section area of the arch, which made the definition of the structure incomplete from a design point of view. The methodology involved finding an optimal horizontal reaction from minimisation of the cost/weight functional, in order to complete the solution for the centre-line profile of a least weight structure. This approach cannot be applied to stand-alone arches, as the horizontal reaction does not affect their centre-line profile and there is no scope for volume/weight minimisation.

As noted by Wang CY and Wang CM [15], the work of Marano *et al* [16] on providing an optimal arch shape, reproduced the same arch profile as given in [13]; however, it did provide an expression for the varying cross-section area of the arch. It also gave a limiting condition for the span of the arch subjected to both the deck and the arch weight, not realising that this condition would always be satisfied, as demonstrated in this paper.

(iii) Discussion

As explained here, arches of least weight are just a special case of constant stress structures. Although the feature of least weight may appear attractive from the point of view of efficiency of material usage, at the same time, it restricts design options, by returning just one 'optimal' span/rise ratio as an outcome. In practice, factors such as the span and span/rise ratio are dictated by variable environmental conditions of the site, and architectural and functional requirements, such as a minimum headroom to be provided by the arch. It is therefore unlikely that a least weight structure could readily satisfy these conditions. The

analytical form-finding methodology proposed here uses span/rise ratios as input variables, and this opens up many design opportunities within the design space.

Whilst minimisation of material weight/cost is the prime objective of structural optimisation, in practice, such a cost is just a fraction of the overall design and construction budget. It is also worth noting that there is a trade-off between minimum weight and durability of the arch. A value of stress associated with permanent load (as advocated here), produces structures optimised for statistically prevalent load; structures analogical to those found in nature. At this point, it is interesting to note that there exists a parallel between constant stress arches and (minimal) constant stress surface structures, as both are subject to limits defining their existence [17, 18].

In all the reviewed work, the use of the ultimate, not permanent, load was suggested in conjunction with permissible stress based on the elastic limit for the material strength. In contemporary structural design, permissible stress has been replaced by design strength, based on the probability that this value would not be exceeded during the lifespan of the structure. As both the applied load and the level of constant stress affect the geometry of the arch (its centre-line profile and cross-section area), using seemingly the same form of equation for the centre-line profile would produce different outcomes.

2. Analytical form finding: asymmetric form of a constant stress arch subjected to permanent load (arch self-weight and deck weight)

(a) Equilibrium equations

Figure 1 (a) shows a general configuration of an asymmetrical arch of span, l, with one of the supports raised vertically by a distance, Δ. The total arch length, measured along its centre-line profile, is C, and its rise, h, appears not at mid-span, but a distance x_a from the left support. The applied load consists of the deck weight, w, per unit span, and the arch self-weight represented by the volumetric weight density, q. In order to accommodate the requirement of constant stress, f, the arch has a varied cross-section area, A, along its length. The arch is smooth and, at the apex, its cross-section area is A_0. The deck can be supported by open spandrel columns, or hangers (in the case of the deck suspended from the arch) that have negligible weight, compared to the weight of the deck and the arch.
As shown in Figure 1(b), the arch is pin-ended, with the vertical reactions at the supports denoted by V_L and V_R respectively, and the equal and opposite horizontal reactions by H. An arbitrary point between O and P has co-ordinates (ξ, η), and arch length, s, measured from O. In general, at a given point P, the internal forces acting on the arch cross-section are: T- axial or thrust/compressive force, S - shear force, and M - bending moment.

The equations of equilibrium for the segment OP are as follows.

Vertical equilibrium:

$$-T\sin\theta + S\cos\theta - wx - \int_0^s qA\, d\sigma + V_L = 0. \tag{2.1}$$

Horizontal equilibrium:

$$-T\cos\theta - S\sin\theta + H = 0. \tag{2.2}$$

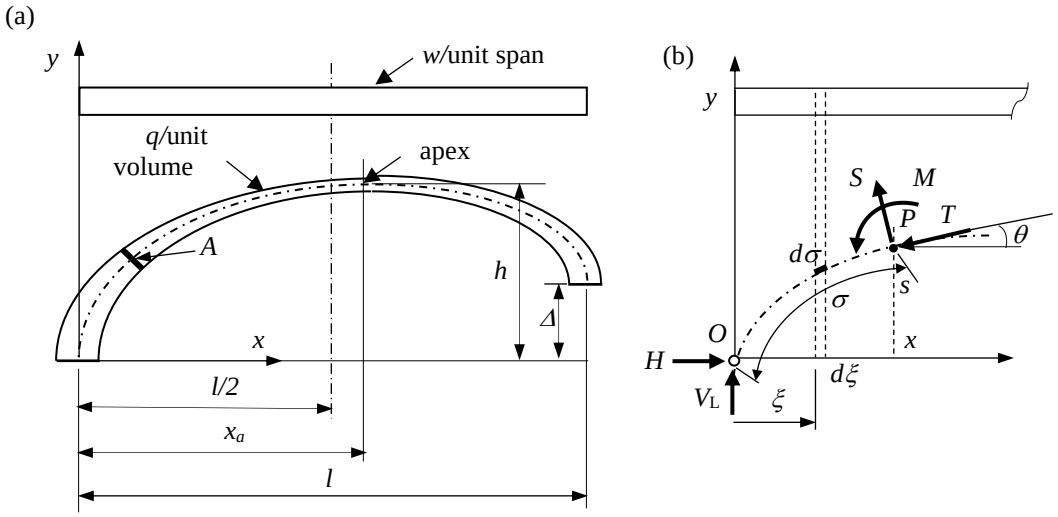

Figure 1 (a) Arch geometry and loading (b) Arch centre-line profile, with its external and internal forces acting on the arch segment *OP*.

Rotational equilibrium about *P*:

$$M + Hy - V_L x + \frac{wx^2}{2} + \int_0^s qA(x - \xi)d\sigma = 0. \tag{2.3}$$

The equations for *S* and *T* are, therefore:

$$\begin{bmatrix} \cos\theta & -\sin\theta \\ \sin\theta & \cos\theta \end{bmatrix} \begin{bmatrix} S \\ T \end{bmatrix} = \begin{bmatrix} wx + \int_0^s qAd\sigma - V_L \\ H \end{bmatrix}.$$

Solving for *S* and *T* gives:

$$S = \cos\theta \left(wx + \int_0^s qAd\sigma - V_L \right) + H\sin\theta\,. \tag{2.4}$$

$$T = -\sin\theta \left(wx + \int_0^s qAd\sigma - V_L \right) + Hcos\theta. \tag{2.5}$$

Differentiating equation (2.3) with respect to *s*, and combining it with the expression for *S* from (2.4), leads to:

$$\frac{dM}{ds} + S = 0. \tag{2.6}$$

This equation of constraint between *M* and *S* has the important consequence that, in a pin-ended arch, the vanishing of shear, *S*, everywhere, is a necessary and sufficient condition for the arch to be moment-less.

(a) Governing differential equation

The vertical reaction V_L can be found by considering rotational equilibrium about the right hand support, from which:

$$V_L = \frac{\Delta}{l}H + \frac{wl}{2} + \frac{1}{l}\int_0^C qA(l-\xi)d\sigma. \tag{2.7}$$

Substituting V_L into (2.4) gives:

$$S = \cos\theta\left[wx + \int_0^s qAd\sigma - \frac{\Delta}{l}H - \frac{wl}{2} - \frac{1}{l}\int_0^C qA(l-\xi)d\sigma\right] + H\sin\theta. \tag{2.8}$$

On using

$$\int_0^C qA(l-\xi)d\sigma = \int_0^s qA(l-\xi)d\sigma + \int_s^C qA(l-\xi)d\sigma$$

and, after grouping the terms, the expression for *S* becomes:

$$S = \cos\theta\left[-w\left(\frac{l}{2}-x\right) - \int_s^C qAd\sigma + \frac{1}{l}\int_0^C qA\xi d\sigma\right] + \left(\sin\theta - \frac{\Delta}{l}\cos\theta\right)H. \tag{2.9}$$

Equating the left hand side of equation (2.9) to zero, and simplifying gives:

$$0 = -w\left(\frac{l}{2}-x\right) - \int_s^C qAd\sigma + \frac{1}{l}\int_0^C qA\xi d\sigma + \left(\tan\theta - \frac{\Delta}{l}\right)H,$$

and since$\tan\theta = y'$, where $y'$is the first derivative with respect to *x*:

$$Hy' = \frac{\Delta}{l}H + w\left(\frac{l}{2}-x\right) + \int_s^C qAd\sigma - \frac{1}{l}\int_0^C qA\xi d\sigma. \tag{2.10}$$

Differentiating equation (2.10) with respect to *x* and noting that:

$$\frac{ds}{dx} = \sqrt{1 + y'^2}$$

gives:

$$y'' = -\left[\frac{w}{H} + \frac{qA}{H}\sqrt{1 + y'^2}\right]. \tag{2.11}$$

Since $S = 0$, then from equation (2.2):

$$T = \frac{H}{\cos\theta} \tag{2.12}$$

and since we also have:

$$T = fA,$$

it follows that:

$$\frac{A}{H} = \frac{1}{f\cos\theta} = \frac{\sqrt{1 + y'^2}}{f}. \tag{2.13}$$

Consequently, the governing non-linear differential equation for the arch centre-line profile, known as the shape equation is:

$$y'' = -\left[\frac{w}{H} + \frac{q}{f}\left(1 + y'^2\right)\right], \tag{2.14}$$

with the boundary conditions:

at $x = 0$, $y = 0$; at $x = l$, $y = \Delta$; at $x = x_a$, $y = h$, and $y' = 0$.

(c) The solution of the governing shape equation

The following transformation of y'' can be used:

$$y'' = \frac{dy'}{dy}\cdot\frac{dy}{dx} = y'\frac{dy'}{dy} = \frac{1}{2}\frac{d}{dy}\left(1 + y'^2\right)$$

and equation (2.14) then becomes:

$$\frac{1}{2}\frac{d}{dy}\left(1 + y'^2\right) = -\left[\frac{w}{H} + \frac{q}{f}\left(1 + y'^2\right)\right]. \tag{2.15}$$

Separating the variables, gives:

$$\frac{f}{2q} ln\left(\frac{w}{H} + \frac{q}{f}\left(1 + y'^2\right)\right) = -y + k_1. \tag{2.16}$$

where k_1 is an arbitrary constant.

At $x = x_a$, $y = h$, and $y' = 0$, which gives:

$$k_1 = h + \frac{f}{2q} ln\left(\frac{w}{H} + \frac{q}{f}\right).$$

It is convenient to introduce parameters:

$$\mu = \frac{q}{f} \tag{2.17}$$

and

$$\kappa = \frac{w}{H} + \mu\,. \tag{2.18}$$

Consequently, equation (2.16) becomes:

$$\frac{1}{2\mu} ln \frac{\kappa + \mu y'^2}{\kappa} = h - y\,,$$

and solving for y' gives:

$$y' = \pm \sqrt{\frac{\kappa}{\mu}(e^{2\mu(h-y)} - 1)}, \tag{2.19}$$

Taking the positive radical and separating the variables in equation (2.19) gives:

$$\int \frac{dy}{\sqrt{e^{2\mu(h-y)} - 1}} = \left(\frac{\kappa}{\mu}\right)^{\frac{1}{2}} x + k_2, \tag{2.20}$$

where k_2 is an arbitrary constant.

Re-writing the left hand side of equation (2.20) gives:

$$\int \frac{dy}{\sqrt{e^{2\mu(h-y)} - 1}} = \int \frac{e^{-\mu(h-y)} dy}{\sqrt{1 - e^{-2\mu(h-y)}}} = \frac{1}{\mu} \text{Sin}^{-1}\left(e^{-\mu(h-y)}\right) = \sqrt{\frac{\kappa}{\mu}} x + k_2.$$

Applying the condition $y = h$ at $x = x_a$ gives:

$$\sin^{-1}(1) = \sqrt{\mu\kappa}\, x_a + k_2 = \frac{\pi}{2}, \tag{2.21}$$

$$k_2 = \frac{\pi}{2} - \sqrt{\mu\kappa}\, x_a.$$

Consequently, the final solution for the centre-line profile of an asymmetric, constant stress arch is:

$$\boldsymbol{y = h + \frac{1}{\mu} \ln \cos(\sqrt{\mu\kappa}\,(x - x_a))} \tag{2.22}$$

where, as shown in section (d) below, x_a is a function of μ, h, and Δ.

The solution presented above relied on $y' > 0$, taken from equation (2.19). It can be readily demonstrated that taking $y' < 0$ leads to the same answer, as given in equation (2.22).

(d) Determination of the unknown parameters and the solution process

In order to determine the centre-line profile of the arch, it is necessary to find the horizontal reaction, H, in terms of the independent input variables (l, h, q, w, and f), as well as the horizontal distance to the apex of the arch, x_a.

Using the condition at the pin: at $x = 0$, $y = 0$:

$$0 = h + \frac{1}{\mu} \ln \cos(\sqrt{\mu\kappa}\,(0 - x_a)),$$

$$\cos(\sqrt{\mu\kappa}\, x_a) = e^{-\mu h}, \tag{2.23}$$

giving:

$$\kappa = \frac{w}{H} + \mu = \frac{1}{\mu {x_a}^2} [\cos^{-1}(e^{-\mu h})]^2.$$

Consequently, the horizontal reaction is:

$$H = \frac{fqw}{\left[\frac{f}{x_a} \cos^{-1}(e^{-\mu h})\right]^2 - q^2}. \tag{2.24}$$

On using the condition $x = l$, $y = \Delta$, the procedure described above can be repeated to give:

$$H = \frac{fqw}{\left[\frac{f}{l - x_a} \cos^{-1}(e^{-\mu(h-\Delta)})\right]^2 - q^2}. \tag{2.25}$$

Equating the right hand sides of equations (2.24) and (2.25) leads to:

$$x_a = \frac{\cos^{-1}(e^{-\mu h})}{\cos^{-1}(e^{-\mu(h-\Delta)}) + \cos^{-1}(e^{-\mu h})}\, l. \tag{2.26}$$

The geometry of the arch is not complete without a knowledge of the distribution of the material along the arch length, described by A_0 and A. From horizontal equilibrium, $\frac{H}{f} = A_0$ and substituting this expression to equation (2.24) gives the cross-section area at the apex:

$$A_0 = \frac{qw}{\left[\frac{f}{x_a}\cos^{-1}(e^{-\mu h})\right]^2 - q^2}. \tag{2.27}$$

The parameter κ in equation (2.18) can be written as:

$$\kappa = \frac{w}{H} + \frac{q}{f} = \frac{q}{f}\left(1 + \frac{w/q}{A_0}\right) = \mu\left(1 + \frac{w/q}{A_0}\right).$$

Inserting the above expression for κ into equation (2.22) and substituting for A_0, gives the following form of that equation:

$$y = h + \frac{1}{\mu}\ln\cos\left(\sqrt{\mu^2\left(1 + \frac{w/q}{A_0}\right)}\,(x - x_a)\right) = h + \frac{1}{\mu}\ln\cos\left[\frac{1}{x_a}\cos^{-1}(e^{-\mu h})(x - x_a)\right], \tag{2.28}$$

from which it can be seen that the centre-line profile is independent of the deck weight, w, as previously stated in [13].

The varying cross-section of the arch, A, is given as:

$$A = \frac{A_0}{\cos\theta} = \sqrt{1 + y'^2}A_0 = A_0\sqrt{1 + \frac{\kappa}{\mu}\tan^2\left[\sqrt{\mu\kappa}\,(x - x_a)\right]}, \tag{2.29}$$

and the volume of the arch, V, is determined as follows:

$$V = \int_0^C A ds = A_0\int_0^l \left[1 + \frac{\kappa}{\mu}\tan^2\left(\sqrt{\mu\kappa}\,(x - x_a)\right)\right]dx$$

$$= A_0 l + \frac{\kappa}{\mu}A_0\int_0^l \left[\sec^2(\sqrt{\mu\kappa}\,(x - x_a)) - 1\right]dx, \tag{2.30}$$

which reduces to:

$$V = \left(1 - \frac{\kappa}{\mu}\right) A_0 l + \frac{\kappa}{\mu\sqrt{\mu\kappa}} A_0 \left[\tan\left(\sqrt{\mu\kappa}\ (l - x_a)\right) + \tan\sqrt{\mu\kappa}\ x_a\right]. \tag{2.31}$$

The solution process requires a suitable value of constant stress, *f*, to be selected, such that stresses in the structure arising from the ultimate (permanent + live) load do not exceed the design strength of the material. For a chosen material, the volumetric weight density, *q*, is known and, therefore, $\mu = q/f$ is known. Since the rise, *h*, is also an independent input variable, the horizontal distance to the apex, x_a, can be determined using equation (2.26). The horizontal reaction, *H*, can then be found from equation (2.24) or (2.25), and κ from (2.18). Finally, equation (2.22) can then be used to find the unknown vertical co-ordinates, *y*, of the centre-line profile of the arch. The geometric description of the arch is not complete without defining its cross- section area at the apex, A_0, and the varied cross-section area, *A*; these can be found from equations (2.27) and (2.28), respectively.

It should be noted that the relationship for A_0 given by equation (2.27), as well as equations (2.24) and (2.25) describing *H*, do not hold for the case $w = 0$, i.e., a stand-alone arch carrying its own weight only. In this case, the cross-section area at the apex, A_0, becomes an independent input variable, and the centre-line profile is independent of both *w* and *H*. Consequently, a stand-alone arch requires a separate treatment, as discussed in the next section.

3. Asymmetric form of a constant stress arch carrying the arch weight only

From equation (2.22) we have:

$$y = h + \frac{1}{\mu} \ln \cos(\sqrt{\mu\kappa}\ (x - x_a),$$

with $\mu = q/f$ and $\kappa = w/H + \mu$, defined earlier.

In the case, when the arch weight is the only load acting on the structure, $w = 0$, and $\kappa = \mu$. Consequently, the equation defining the centre-line profile of the arch is:

$$y = h + \frac{1}{\mu} \ln \cos[\mu(x - x_a)], \tag{3.1}$$

with x_a defined in equation (2.26).

The above equation shows that the horizontal reaction, *H*, plays no role in describing the centre-line profile of the arch, and the cross-section area at the apex, A_0, becomes an independent input variable defining the size of the arch, and hence the load, acting on the structure. With A_0 assumed, the horizontal reaction is:

$$H = A_0 f \tag{3.2}$$

and the cross-section area varying along the span is:

$$A = \frac{A_0}{\cos\theta} = \sqrt{1 + y'^2} A_0 = A_0 \sqrt{1 + \tan^2(\mu\ (x - x_a))}. \tag{3.3}$$

With $w = 0$, $\kappa = \mu$, and using equation (2.30), the volume of an asymmetric constant stress arch subjected to arch weight only becomes:

$$V = \frac{1}{\mu} A_0 \left[\tan\left(\mu\,(l - x_a)\right) + \tan \mu\, x_a\right]. \tag{3.4}$$

4. Symmetric form of a constant stress arch subjected to permanent load (arch self-weight and deck weight)

(a) Centre-line profile and the determination of the unknown, dependent parameters

The arch becomes symmetric, when $x_a = l/2$ and $\Delta = 0$. With the origin moved to the centre of the arch, equation (2.22) gives the centre-line profile for a symmetric arch of constant axial stress, as:

$$\boldsymbol{y = h + \frac{1}{\mu} \ln \cos(\sqrt{\mu\kappa}\, x)}. \tag{4.1}$$

Since $\cos(\sqrt{\mu\kappa}\, x) < 1,\ \ln\cos(\sqrt{\mu\kappa}\, x) < 0$.

It was stated earlier, that the centre-line profile is independent of the deck weight density, *w*. Here, substituting $x_a = \frac{l}{2}$ in equation (2.28) gives:

$$y = h + \frac{1}{\mu} \ln \cos\left[\frac{2}{l} cos^{-1}(e^{-\mu h})(x)\right]. \tag{4.2}$$

Using the condition at the pin: at$x = l/2\ ,\ y = 0$, equation (4.1) gives:

$$0 = h + \tfrac{1}{\mu} \ln \cos(\sqrt{\mu\kappa}\ \tfrac{l}{2}),$$

and the constraint condition given previously by equation (2.23) becomes:

$$\cos(\sqrt{\mu\kappa}\, \frac{l}{2}) = \ e^{-\mu h}. \tag{4.3}$$

Equations (2.24) and (2.25) describing the horizontal reaction, *H*, collapse to just one equation:

$$H = \frac{fqw}{\left[\frac{2f}{l}\cos^{-1}(e^{-\mu h})\right]^2 - q^2}. \tag{4.4}$$

Equation (2.27) describing the cross-section area at the apex now becomes:

$$A_0 = \frac{H}{f} = \frac{qw}{\left[\frac{2f}{l}\cos^{-1}(e^{-\mu h})\right]^2 - q^2}, \tag{4.5}$$

giving the varying cross-section area:

$$A = A_0\sqrt{1+\frac{\kappa}{\mu}\tan^2\left(\sqrt{\mu\kappa}\ x\right)}. \tag{4.6}$$

Using equation (2.31), and noting that $x_a=l/2$, the volume of the symmetric form of a constant stress arch subjected to the arch and deck weight is:

$$\begin{aligned} V &= \left(1-\frac{\kappa}{\mu}\right)A_0 l + \frac{\kappa}{\mu\sqrt{\mu\kappa}}A_0\left[\tan\left(\sqrt{\mu\kappa}\ \frac{l}{2}\right)+\tan\left(\sqrt{\mu\kappa}\ \frac{l}{2}\right)\right] \\ &= 2A_0\left[\left(1-\frac{\kappa}{\mu}\right)\frac{l}{2}+\sqrt{\frac{\kappa}{\mu^3}}\tan\left(\sqrt{\mu\kappa}\ \frac{l}{2}\right)\right]. \end{aligned} \tag{4.7}$$

(b) Apparent constraint on the span of a constant stress arch

The arch length, *C*, (measured by the arc along the centre-line profile) is given as:

$$C = 2\int_0^{l/2}\sqrt{1+y'^2}\,dx = 2\int_0^{l/2}\sqrt{\left(1+\frac{\kappa}{\mu}\tan^2\left(\sqrt{\mu\kappa}\,x\right)\right)}\,dx, \tag{4.8}$$

which gives the following form for the arch length:

$$C = 2\int_0^{l/2}\frac{\sqrt{\cos^2\sqrt{\mu\kappa}x+\frac{\kappa}{\mu}\sin^2\sqrt{\mu\kappa}x}}{\cos\sqrt{\mu\kappa}x}\,dx.$$

Using $t=\sin\sqrt{\mu\kappa}x$, $dt=\sqrt{\mu\kappa}\cos\sqrt{\mu\kappa}x dx$, leads to:

$$C = 2\int_0^{\sin\sqrt{\mu\kappa}\frac{l}{2}}\frac{\sqrt{1+\left(\frac{\kappa}{\mu}-1\right)t^2}}{1-t^2}\,dt. \tag{4.9}$$

It can be shown that, if$\sin\left(\sqrt{\mu\kappa}\,\frac{l}{2}\right)=1$, the integral becomes improper and the arch length unbounded, which suggests that the following relationship should hold:

$$\sqrt{\mu\kappa}\frac{l}{2} = \frac{q}{f}\sqrt{\left(\frac{w}{qA_0}+1\right)}\frac{l}{2} = \frac{ql}{2f}\sqrt{\left(\frac{w}{qA_0}+1\right)} < \frac{\pi}{2}\ . \tag{4.10}$$

The above formula has been derived in [16]. However, a further study reveals that the inequality given in (4.10) will always be satisfied, as demonstrated below.

Equation (4.5) can be re-written as:

$$A_0 = \frac{qw}{q^2 \left\{ \left[\frac{2f}{ql} \cos^{-1}(e^{-qh/f}) \right]^2 - 1 \right\}}. \tag{4.11}$$

It is helpful to introduce non-dimensional quantities, γ and ρ, as shown below:

$$\gamma = \frac{ql}{2f}, \tag{4.12}$$

and the span/rise ratio:

$$\rho = \frac{l}{h}. \tag{4.13}$$

Also noting that:

$$\frac{qh}{f} = \frac{ql}{f\rho} = 2\frac{ql}{2f\rho} = \frac{2\gamma}{\rho},$$

gives:

$$A_0 = \frac{w}{q \left\{ \left[\frac{1}{\gamma} \cos^{-1}(e^{-2\gamma/\rho}) \right]^2 - 1 \right\}}. \tag{4.14}$$

Substituting equation (4.14) into (4.10) gives:

$$\gamma \sqrt{[1 + \{\cos^{-1}(e^{-2\gamma/\rho})/\gamma)\}^2 - 1]} < \frac{\pi}{2},$$

that is:

$$\cos^{-1}(e^{-2\gamma/\rho}) < \frac{\pi}{2}. \tag{4.15}$$

As $e^{-2\gamma/\rho}$ is never zero, the limit given by (4.10) will always be satisfied. In practice, however, the arch length would become increasingly large as $e^{-2\gamma/\rho} \to 0$.

(c) Constraint conditions determining the existence of the constant stress arch

Equation (4.4) can be re-written as:

$$H = \frac{wf}{q\left[\frac{1}{\gamma}\cos^{-1}(e^{-2\gamma/\rho})\right]^2 - 1} = \frac{rf}{\left[\frac{1}{\gamma}\cos^{-1}(e^{-2\gamma/\rho})\right]^2 - 1} \tag{4.16}$$

where $r = w/q$.

Consequently, equation (4.14) becomes:

$$A_0 = \frac{H}{f} = \frac{r}{\left[\frac{1}{\gamma}\cos^{-1}(e^{-2\gamma/\rho})\right]^2 - 1}. \tag{4.17}$$

It can be seen from equation (4.16) that the horizontal reaction, *H*, derived from the end condition, can become negative, when:

$$\left[\frac{1}{\gamma}\cos^{-1}\left(e^{-2\gamma/\rho}\right)\right]^2 < 1, \tag{4.18}$$

and $H = \infty$ when

$$\cos^{-1}\left(e^{-2\gamma/\rho}\right) = \gamma. \tag{4.19}$$

Consequently, it can be seen from equation (4.17) that $A_0 < 0$ when inequity (4.18) holds, or $A_0 \to \infty$ when the equation (4.19) is satisfied. Equation (4.19) may be re-written as:

$$e^{-2\gamma/\rho} = \cos\gamma\,,$$

leading to a critical relationship between ρ and γ, given by:

$$\rho = \frac{2\gamma}{\ln\sec\gamma}. \tag{4.20}$$

When the above relationship holds, A_0 becomes unbounded, as does the horizontal reaction, *H*. Equation (4.20) also indicates that $ln\sec\gamma$ must not become infinitely large, and for this to happen, the following inequality must be satisfied:

$$\gamma = \frac{ql}{2f} < \frac{\pi}{2} \tag{4.21}$$

The condition given in (4.21) has been given in [13] in relation to 'fully stressed' or least weight arches, but equation (4.20) is a new result, the significance of which merits a further analysis. It is shown (Appendix A) that when the span/rise ration, ρ, falls outside the ρ - γ curve, i.e.,

$$\rho > \frac{2\gamma}{\ln\sec\gamma}\,,$$

both the horizontal reaction, *H*, and the cross-section area at the apex, A_0, become negative (equations (4.15) and (4.16), respectively). In view of this, the critical $\rho - \gamma$ curve, shown in figure 2, determines the boundary of the area within which ρ and γ can be chosen. For the points lying on the curve, the horizontal reaction, *H*, and the cross-section area at the apex, A_0, become infinitely large; for the points above the curve, they acquire negative values.

Detailed calculations of the $\rho - \gamma$ limits related to specific spans for both concrete and steel structures, are given in electronic supplementary material S1.

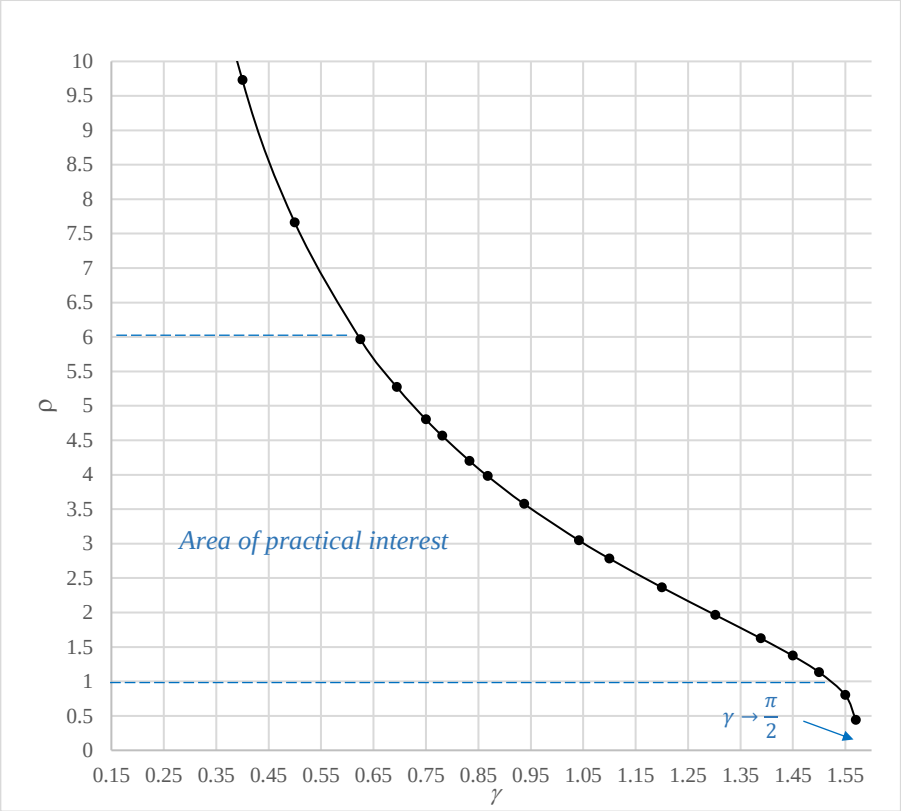

Figure 2 Limiting $\rho - \gamma$ relationship defining the design space/existence of a constant stress arch

Figure 2 illustrates conditions for the existence of a constant stress arch, given in terms of two dimensionless parameters: ρ and γ. It can be seen that **the limit $\gamma < \pi/2$ is a necessary, but not sufficient condition for ensuring the existence of a constant stress arch**. **The area under the curve represents the available design space for arbitrary ρ - γ combinations.**

As stated in Section 1, there exists an interesting parallel between constant stress arches and (minimal) constant stress surfaces; more specifically, stable minimal surfaces, exemplified by soap films [17], [18]; both of these structures are subject to conditions limiting their existence. For example, it is known that a catenoid surface – a surface formed between two co-axial rings (one of the few minimal surfaces that have a closed-from solution) cannot be formed when the ratio of the ring separation to their radius is greater than 1.325. Of course, infinitely many catenoids, of different ring separations and radii, satisfying the stated limit, can be formed.

(d) Span/rise ratio minimising the volume of material

From equation (4.6) we have:

$$V = 2A_0\left[\left(1-\frac{\kappa}{\mu}\right)\frac{l}{2}+\sqrt{\frac{\kappa}{\mu^3}}\tan\left(\sqrt{\mu\kappa}\ \frac{l}{2}\right)\right]$$

It is helpful to write:

$$\kappa = \frac{qA_0}{H}\left(1+\frac{w}{qA_0}\right) = \frac{q}{f}\left(1+\frac{r}{A_0}\right), \tag{4.22}$$

where $r = w/q$, defined earlier.

Introducing a non-dimensional parameter z:

$$z = \gamma\sqrt{1+\frac{r}{A_0}} \tag{4.23}$$

and with $\mu = \frac{q}{f}$ defined earlier, and κ defined in (4.22), we get:

$$\frac{\kappa}{\mu} = \frac{z^2}{\gamma^2}$$

$$1-\frac{\kappa}{\mu} = 1-\left(1+\frac{r}{A_0}\right) = -\frac{r}{A_0}$$

$$\sqrt{\mu\kappa} = \frac{q}{f}\sqrt{1+\frac{r}{A_0}} = \frac{2}{l}z,$$

$$\sqrt{\frac{\kappa}{\mu^3}} = \frac{l}{2\gamma^2}z\ ,$$

giving the expression for the volume (equation (4.7)):

$$V = 2A_0\left[-\frac{r}{A_0}\cdot\frac{l}{2}+\frac{lz}{2\gamma^2}\tan z\right] = rl\left[-1+\frac{zA_0}{\gamma^2 r}\tan z\right]. \tag{4.24}$$

Since:

$$\gamma^2\left(1+\frac{r}{A_0}\right) = z^2$$

$$\frac{r}{A_0} = \frac{z^2-\gamma^2}{\gamma^2},$$

equation (4.24) becomes:

$$V = rl\left[-1+\frac{z}{z^2-\gamma^2}\tan z\right]. \tag{4.25}$$

The constraint condition given by equation (4.3), re-written in terms of γ, and ρ is:

$$\cos z = e^{-2\gamma/\rho}, \tag{4.26}$$

from which:

$$\frac{dz}{d\rho} = -\frac{2\gamma e^{-\frac{2\gamma}{\rho}}}{\rho^2\sqrt{1-e^{-\frac{2\gamma}{\rho}}}}. \tag{4.27}$$

Minimising volume given in (4.25) with respect to ρ gives:

$$\frac{dV}{d\rho} = 0 = rl\left[\frac{(z^2-\gamma^2)-2z^2}{(z^2-\gamma^2)^2}\tan z + \frac{z}{z^2-\gamma^2}\sec^2 z\right]\frac{dz}{d\rho}.$$

Since $\frac{dz}{d\rho}$ is non-zero, the equation minimising the arch volume is:

$$\tan^2 z - \frac{z^2+\gamma^2}{z(z^2-\gamma^2)}\tan z + 1 = 0, \tag{4.28}$$

and the solution to it, say $\bar{z}$, can be obtained using a number of numerical methods.

With $\bar{z}$ determined from equation (4.28), the span/rise ratio, $\rho_{\min}$, at which the arch becomes a structure of least weight, is:

$$\rho_{\min} = -\frac{2\gamma}{\ln\cos\bar{z}}\ . \tag{4.29}$$

Results of the above analysis for the arch made of concrete are summarised in Table 1. The full set of results is given in electronic supplementary material S2. It can be seen that, in the case f =1.5MPa, and γ = 1.6667, the span/rise ratio, $\rho_{\min}$, is not reached, because the condition given by equation (4.21) is violated, i.e., $\gamma > \pi/2$.

Table 1 Values of span/rise ratio, $\rho_{\min}$ and $\bar{z}$

	l = 50 m			l = 100 m			l = 150 m			l = 200 m		
f	γ	$\bar{z}$	$\rho_{\min}$	γ	$\bar{z}$	$\rho_{\min}$	γ	$\bar{z}$	$\rho_{\min}$	γ	$\bar{z}$	$\rho_{\min}$
(1)	(2)	(3)	(4)	(5)	(6)	(7)	(8)	(9)	(10)	(11)	(12)	(13)
3.6 MPa	0.1736	0.5431	2.23	0.3472	0.7616	2.15	0.5208	0.9257	2.05	0.6944	1.0618	1.93
2.4 MPa	0.2604	0.6623	2.19	0.5208	0.9256	2.05	0.7813	1.1229	1.87	1.0417	1.2873	1.64
1.8 MPa	0.3472	0.7616	2.15	0.6944	1.062	1.93	1.0417	1.2873	1.64	1.3889	1.4782	1.17
1.5 MPa	0.4167	0.8316	2.11	0.8333	1.1578	1.64	1.25	1.4046	1.39	1.6667	Not available	Not available

Using an example of a constant stress arch of span l = 50 m, and the following additional input parameters: w = 50 kN/m, q = 25 kN/m^3 (corresponding to concrete weight density), the volume of the arch can be calculated from equation (4.7), or (4.25), for a range of span/rise ratios and stress values. The results are presented in figure 3, with detailed calculations given in supplementary electronic material S2.

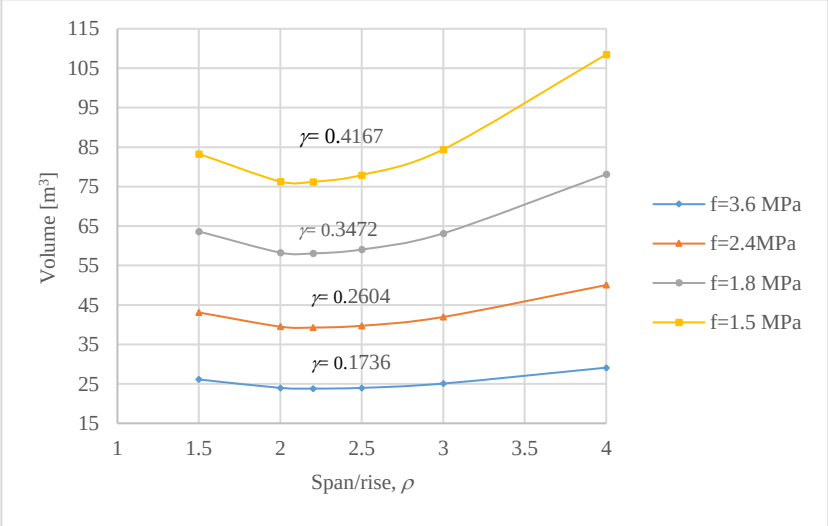

Figure 3 Variation of volume with span/rise ratio, ρ, and a range of γ and corresponding to chosen values of constant stress, f. Other data: q =25kN/m^3 and span l = 50m.

With reference to figure 3, it can be seen that, for a given span and stress (corresponding to specific values ofγ), the span/rise ratio minimising the volume of the material in the arch is ρ_{min} is just above 2. The more exact values for ρ_{min} are given in column 4 of Table 1. A similar study can be carried out for other spans, as shown in Table 1, and for steel structures, with q = 75 kN/m^3 and a range of stress appropriately scaled up.

Each curve in figure 3 represents a family of constant stress arches that can be generated within a given span, l, depending on the chosen span/rise ratio, ρ, and value of stress, f. It can be checked that this family falls safely into the design space given in figure 2. Figure 3 indicates that the arch volume is influenced by the value of stress. Figure 4 shows that stress has only a small effect on the centre-line profile of the arch, and hence, the change in volume is largely due to the cross-section area being affected.

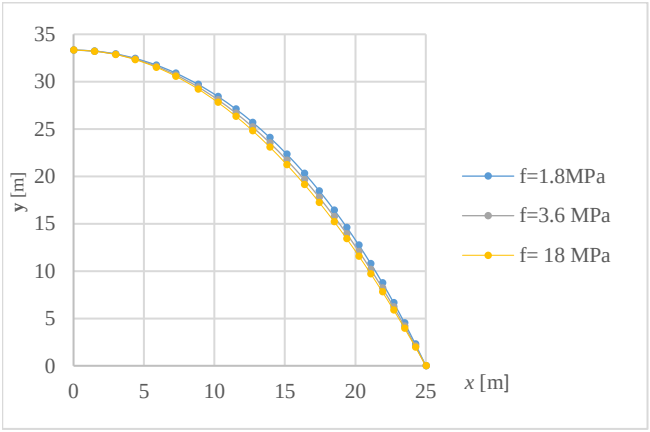

Figure 4 Centre- line profiles for varying values of constant stress, f, and ρ =1.5

5. Symmetric form of a constant stress arch subjected to arch weight only: the stand-alone arch

(a) Centre-line profile

With the deck weight, $w = 0$, $\kappa = w/H + q/f = \mu$, the centre-line equation (4.1) becomes:

$$\boldsymbol{y = h + \frac{1}{\mu} \ln \cos \mu x}, \tag{5.1}$$

where, for a bounded solution, $\mu \frac{l}{2} < \frac{\pi}{2}$.

It can be seen from equation (5.1) that the horizontal reaction, *H*, plays no role in determining the centre-line profiles of the arch. Consequently, it is not possible to find a value of *H* that minimises the arch weight/volume that the structural optimisation methodology relies on.

(b) Remaining design parameters

As stated in Section 2(d) the apex cross-section of the arch, A_0, can no longer be determined from the equations given for the fully loaded arch, as it now becomes an independent variable. With A_0 selected, the horizontal reaction is given by equation (3.2) and the varying cross section, *A*, is:

$$A = \frac{A_0}{\cos \theta} = \sqrt{1 + y'^2} A_0 = A_0 \sqrt{1 + \tan^2(\mu x)}. \tag{5.2}$$

The volume of the arch can be found from equation (4.7), which, on substitution $\kappa = \mu$, gives:

$$V = 2 \frac{A_0 l}{\mu} \tan(\mu \frac{l}{2}), \tag{5.3}$$

or, since $\gamma = \frac{ql}{2f} = \mu \frac{l}{2}$

$$V = \frac{A_0 \, l}{\gamma} \tan \gamma. \tag{5.4}$$

In the case of a fully loaded arch, the volume of the arch was dependent on span, *l*, as well as the span/rise ratio, ρ, and γ (corresponding to the chosen stress, *f*). As can be seen from equation (5.4), the volume of a stand-alone arch is independent of the span/rise ratio; it depends only on *l* and γ, with A_0 acting as a scaling factor. Figure 5 shows the relationship for a small, stand-alone arch, with A_0 taken as unity. It can be seen that as $\gamma \to \frac{\pi}{2}$, the volume increases without limit.

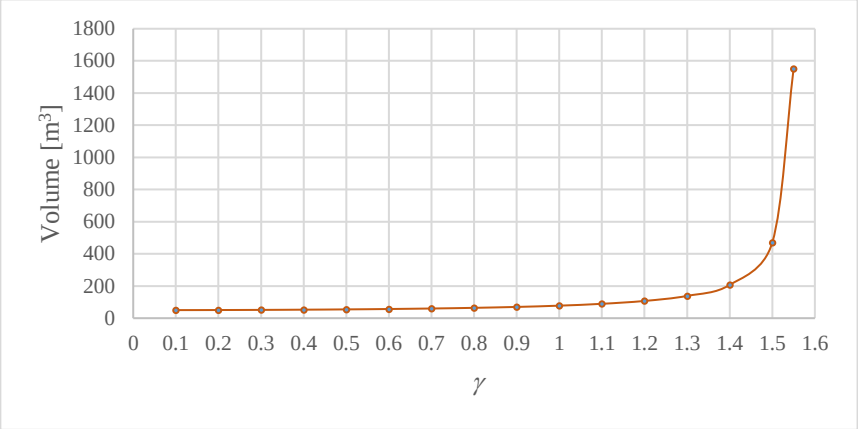

Figure 5 Volume of a stand-alone arch as a function of γ; A_0 taken as unity, span l =50 m

(c) Constraint condition

Implementing the end condition: $x = l/2$, $y = 0$, gives:

$$0 = h + \frac{1}{\mu}\ln\cos(\mu\frac{l}{2}), \tag{5.5}$$

or

$$e^{-\mu h} = \cos(\mu\frac{l}{2}) = \cos(\frac{q}{f}\frac{l}{2}) = \cos\gamma.$$

which, in terms of ρ and γ becomes:

$$e^{-2\gamma/\rho} = \cos\gamma\,, \tag{5.6}$$

or:

$$\rho = \frac{2\gamma}{\ln sec\,\gamma}\,. \tag{5.7}$$

Equation (5.7) is of the same form as equation (4.21), which marked the boundary of the available design space for arbitrarily chosen ρ and γ, in the case of a fully loaded arch. Here, the same equation has a different significance; it shows that, for a given ρ, there can be only one value of γ. Thus, for a chosen material characterised by its weight density, q, and given span, l, there exists a unique relationship between ρ and stress, f. As ρ is the input parameter, the required value of stress can be found as shown below.

From equation (5.5) we have:

$$0 = h\mu + \ln\cos(\mu\frac{l}{2}).$$

Introducing $u = \mu l/2$ and noting that $h\mu = \frac{l}{\rho}\cdot\frac{2u}{l}$, we get:

$$0 = \frac{2u}{\rho} + \ln \cos u. \tag{5.8}$$

Solving the above equation for u, gives μ that can be used to: (i) determine the required value of constant stress, $f = q/\mu$, and (ii) find the y co-ordinates of the arch from equation (5.1). Detailed calculation for f is given in the electronic supplementary material S3.

Figure 6 shows a 1:20 model of a small, stand-alone, constant stress arch, created using the following input variables: l = 6 m, ρ = 1, A_0 = 0.3 m^2. The arch has a square cross-section varying along the arch length. It is found that the stress required to satisfy equation (5.7) is 0.049 MPa. Detailed calculations of the arch centre-line profile and volume are given in electronic supplementary material S3.

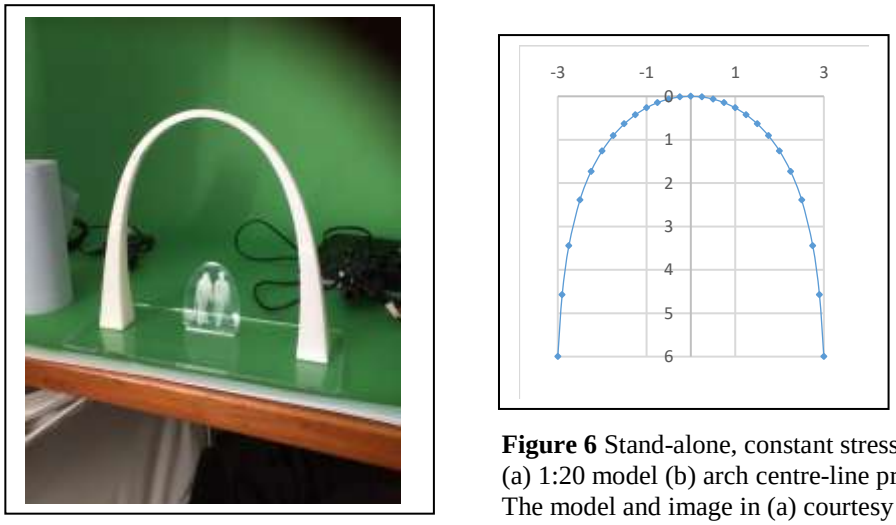

Figure 6 Stand-alone, constant stress arch (a) 1:20 model (b) arch centre-line profile. The model and image in (a) courtesy of M. Millson, University of Warwick

6. Summary and conclusions

This paper presents an analytical form-finding methodology describing 2-pin, moment-less arches, shaped by a constant value of axial stress developing under statistically prevalent (permanent) load. The methodology employed is that of analytical form-finding, in which an arch of a given span and rise is shaped by the applied loads and a chosen value of constant stress. The resulting forms of arches are close to natural objects characterised by a minimal stress response to applied load.

Compared to optimisation approaches concerned with least weight structures, the proposed methodology, defining constant stress arches, opens up design opportunities by offering not one, but a range of optimal span/rise ratios, provided they fall into the available design space - a new concept derived here. The results show that an apparent limit on span of least weight arches is always satisfied, although structures approaching this limit are unlikely to meet practical requirements. In the case of a stand-alone arch, the design space reduces to that of a constraint relationship between the span/rise ratio and constant stress.

The proposed analytical form-finding methodology describes a general case of an asymmetric, constant stress arch, from which a symmetric form is deduced. The profile of the stand-alone arch is obtained from the general case of a fully loaded structure by setting the deck weight to zero. The case of a stand-alone arch, successfully solved by the proposed

method, proved to lie outside the scope of structural optimisation aimed at least weight arches.

Constant stress arches are efficient structures, because of their simple stress response to loading, but they are not necessarily structures of least weight. It is shown here that arches of least weight are just a special case of constant stress forms, as demonstrated by the derivation of an explicit solution for the span/rise ratio minimising the arch volume.

It is confirmed that the deck weight does not influence the centre-line profile; instead, it affects material distribution in the arch and, consequently its volume. An important design factor in the proposed methodology is the level of constant stress. When its value corresponds to the ultimate load, the solution represents an optimum just for this transient load, with the structure working in non-optimal state under permanent load. The proposed analytical form-finding approach advocates the use of permanent load, assumed to be statistically prevalent, to ensure that the structure works in an optimal state most of the time. Further work is needed to establish an appropriate level of constant stress, so that the arch does not exceed design strength limits when subjected to ultimate load, or becomes too heavy, when the chosen value of stress is too low.

Appendix A

Here, it will be shown that the horizontal reaction, *H*, and, consequently, the cross-section area at the apex, $A_{0,}$ become negative, if the span/rise ratio, $\bar{\rho}$, is chosen to lie above the bounding curve in figure 2.

For some $\lambda > 1$, we choose $\bar{\rho}$ as:

$$\bar{\rho} = \lambda \frac{2\gamma}{\ln \sec \gamma}.$$

Then, the denominator in equations (4.15) and (4.16) becomes:

$$\left[\frac{1}{\gamma}\cos^{-1}\left(e^{-\frac{2\gamma}{\bar{\rho}}}\right)\right]^2 - 1 = \left[\frac{1}{\gamma}\cos^{-1}\left(e^{-\frac{2\gamma}{\frac{2\gamma\lambda}{\ln\sec\gamma}}}\right)\right]^2 - 1 =$$

$$= \left[\frac{1}{\gamma}\cos^{-1}\left(e^{-\frac{1}{\lambda}\ln\sec\gamma}\right)\right]^2 - 1 = \left[\frac{1}{\gamma}\cos^{-1}\left(e^{\ln(\cos\gamma)^{\frac{1}{\lambda}}}\right)\right]^2 - 1 =$$

$$= \left[\frac{1}{\gamma}\cos^{-1}\left((\cos\gamma)^{\frac{1}{\lambda}}\right)\right]^2 - 1.$$

Since $\cos\gamma < 1$, and $\lambda > 1$, $(\cos\gamma)^{\frac{1}{\lambda}} > \cos\gamma$. Choosing $\cos\alpha = (\cos\gamma)^{\frac{1}{\lambda}}$, then $\cos\alpha > \cos\gamma$, and $0 < \alpha < \gamma$. Consequently,

$$\left[\frac{1}{\gamma}\cos^{-1}\left(e^{-\frac{2\gamma}{\bar{\rho}}}\right)\right]^2 - 1 = \left[\frac{1}{\gamma}\cos^{-1}(\cos\alpha)\right]^2 - 1 = \left(\frac{\alpha}{\gamma}\right)^2 - 1 < 0,$$

and it follows that *H* and A_0 become negative.

Data accessibility. Geometrical and stress analyses data is provided in the electronic supplementary material.
Competing interests. There are no competing interests.
Funding. No external funding was used to support this work.

References

1. Lewis WJ. 2016. Mathematical model of a moment-less arch. *Proc. R. Soc,* A 472, (doi: 10.1098/rspa.2016.0019).
2. Mattheck C. 1998. *Design in nature. Learning from trees.* Berlin Heidelberg: Springer Verlag.
3. Otto F. and Rasch B. 1995. *Finding form: towards an architecture of the minimal*. Deutscher Vergbund Bayern. Edition Axel Menges.
4. Lewis WJ. 2018. *Tension structures: form and behaviour*. 2nd ed. ICE Publishing, London.
5. Gilbert D. 1826. On the mathematical theory of suspension bridges, with tables for facilitating their construction. *Phil. Trans. R. Soc. Lond*. 116, 202-218.
6. Calladine CR. 2014. An amateur's contribution to the design of Telford's Menai suspension bridge: a commentary on Gilbert (1826) 'On the mathematical theory of suspension bridges'. *Phil. Trans. R. Soc. A* 373: 2014346.
7. Routh EJ. 1896. A treatise on analytical statics: with numerous examples. Vol. 1. Cambridge University Press, 2013.
8. Williams C. 2014. What is a shell? In *Shell structures for architecture*. *Form finding and optimization.* Editors: Adriaenssens et al, Routledge, 28-30.
9. Moseley H. 1855. *The Mechanical principles of engineering and architecture*. 2nd edn. London. Brown, Green & Longmans UK.
10. Rozvany GIN, Wang C, Dow M. 1981. Prager-structures: archgrids and cable networks of optimal layout. *Comp. Meth. Appl. Mech and Engng*. 3, 91-113. North Holland Publishing Company.
11. Maxwell JC. 1872. On reciprocal figures, frames and diagrams of forces. *Trans. R. Soc. Edinburgh.* 26, 1-40.; ibid., Scientific papers, Vol 2 , Cambridge University Press, 1890, 161-207
12. Mitchell AGM. 1904. The limits of economy of material in frame structures. *Phil. Mag*. S6, 8, 589-597.
13. Hill RD, Rozvany GIN, Wang CM. 1979. Optimisation, spanning capacity and cost sensitivity of fully stressed arches. *J. Struct. Me*ch. 7:4, 375-410.
14. Wang CM, Rozvany GIN. 1983. On plane Prager structures II: Non-parallel loads and allowances for self-weight. *Int. J. Mech. Scie*. 25: 7, 529-541.
15. Wang CY, Wang CM. 2015. Closed-form solutions for funicular cables and arches. *Acta Mech.* 226, 1641-1645.
16. Marano GC, Trentadue F, Petrone F. 2014. Optimal arch shape solution under static vertical loads. *Acta Mech*. 225, 679-686.
17. Isenberg C. 1978. *The science of soap films and soap bubbles*. Tieto Ltd.
18. Hildebrandt S, Stevens GP. 1985. *Mathematics and optimal form*. Scientific American Library, USA.